Journal of the Nigerian Association of Mathematical Physics
Volume 31, **(July,** *2015***), pp 419 – 428**

A Study of Injectivity Decline of Wells in a Reservoir Intersected By a Fluid Injector

[1]Odeh I.O. , [2]Giegbefumwen P.U. and [3]Adewole E.S

[1,2,3]Department of Petroleum Engineering, University of Benin, Nigeria.

Abstract

Reliable prediction of injectivity decline from an injection well history provides adequate information for better planning of water treatment and well stimulation procedures for an injection programme. The accuracy of such predictions is strongly dependent on the applied model. To this regard, this work presents a systematic study of injectivity decline forecast by providing a numerical solution to the convection-diffusion pressure model for injectivity decline prediction during internal particle filtration from produced water reinjection (PWRI).

Results obtained from the implicit finite difference solution to the model showed the existence of a linear relationship between average formation porosity and permeability, as well as porosity reduction around the invaded zone during water injection. Furthermore, a study on cake development due to external filtration showed a steady increase in cake thickness around the invaded reservoir region leading to more impedance to injectivity and overall injectivity decline.

The similarity in the results obtained in this work and field observations therefore validates the suitability of the convection-diffusion pressure model [1] for the accurate prediction of injectivity decline during produced water reinjection PWRI, and also its usefulness in improving the accuracy of various existing models in the literature which are based on assumed or constant porosity values.

Keywords: produced water reinjection; convection diffusion model; implicit finite difference solution; prediction; injectivity decline; numerical model

Nomenclature

C = particle concentration in the fluid, ppm
λ = filtration coefficient, 1/cm
$\tilde{}_i$ = initial porosity
K = formation permeability, md
K_z = Kozeny constant
K_i = initial permeability, md
$\tilde{}_m$ = porosity of the medium
q = flowrate, c.c/day
A = cross-sectional area, cm^2
Δ_t = time step, days
D_o = molecular diffusion coefficient
C_f = formation compressibility, 1/pa
μ_s = suspension viscosity, pa*s
r = radial distance, cm
β = formation damage factor
h = formation thickness, cm
r_f = radius of injection front, cm
α = ratio of injectivity at time t to initial injectivity
a_L = longitudinal dispersivity

ρ_s = particle density, kg/cc
C_i = particle concentration at the start of the time step, ppm
e_c = cake thickness, cm
$\tilde{}_c$ = porosity of the cake
$\tilde{}^*$= critical porosity value
t_D= dimensionless time
r_e = drainage radius, cm
σ = particle retention coefficient, vol/vol
D = particle dispersion coefficient, cm^2/s
K_D = dimensionless permeability
n = exponent
U = permeate velocity, cm/s
K_o= original formation permeability
T_{tr}= transition time, sec
J = particle flux, cm/s
T= injection time, sec
r_w = wellbore radius, cm
C_p = volume of deposited particles per unit bulk volume

Corresponding author: Odeh I.O., E-mail: odehisaac14@yahoo.com, Tel.: +234-8089566420 & 8038700814(G.P.U)

1.0 Introduction

The cost of treating a candidate water for an injection programme can be quite alarming, especially in the case of an offshore project where the target reservoir has been intercepted by a long horizontal well. As such, little emphasis to injection water treatment is usually given in a bid to minimise the overall cost of the injection project. This often leads to a situation where Injectivity decline during sea water injection or produced water reinjection PWRI becomes a wide spread catastrophe. The problem of injectivity impairment is due in part to internal particle filtration during sea water/produced water reinjection and partly to external cake development in the surface of the well due to build-up of filtered particles from the injected water.
This work presents a systematic study of injectivity decline forecast by providing the numerical solution to the convection-diffusion pressure model [1].

2.0 Mathematical Model

The unsteady state radial transport equation below, describing the spatial and temporal variation of injection pressure in a homogeneous porous media undergoing advection and dispersion is derived from the mass conservation equation for suspended and retained particles for an incompressible fluid [1]

$$\frac{\partial^2 p}{\partial r^2} + \lambda \frac{\partial p}{\partial r} = \frac{\phi_m}{D} \frac{\partial p}{\partial t} \quad (1)$$

Other models were also employed in actualising our result. Some of these models include:

- **Equation for Hydrodynamic Dispersion**

Hydrodynamic dispersion denotes the spreading at macroscopic level resulting from both mechanical dispersion and molecular diffusion. The equation for hydrodynamic dispersion including molecular diffusion and mechanical dispersion is given by Van Genuchten [2], as

$$D = D_0 \tau + \alpha_L V^n \quad (2)$$

Where, D_o is the molecular diffusion coefficient taken as (1.5×10^{-9} cm^2/sec), v is the interstitial velocity, τ is the tortuosity of the porous medium and D is the longitudinal dispersion coefficient, α_L is the longitudinal dispersivity and n is an exponent. Assuming Peclet number [3] to be in the range of 3.2 - 5.8×10^6, i.e. larger than 6, mechanical dispersion is dominant and the first term on the right hand side of Eq. (2) vanishes. For purpose of this research, D was taken as 0.0006005 cm^2/s.[4]

- ***Equation for Retention Kinetics.***

The kinetic equation which describes the rate of transfer of particles to the porous medium [5] is given by;

$$\frac{\partial \sigma}{\partial t} = \lambda J \quad (3)$$

The particle flux J is characterised by the advective and dispersive components:

$$J = uc - D \frac{\partial c}{\partial r} \quad (4)$$

The calculations by Altoe et al [6] of the number of captured particles per unit time during flow via a sieve sequence shows that capture rate is proportional to the total particle flux . But in one study particle dispersion was taken into account in deep bed filtration modelling [5]. The dispersion term was included in the particle balance but was not accounted for in the capture rate equation. In this work, the particle capture rate is taken to be directly proportional to the total particle flux comprising of both the advection and dispersive components; i.e.

$$\frac{\partial \sigma}{\partial t} = \lambda \left(uc - D \frac{\partial c}{\partial r} \right) \quad (5)$$

- ***Filtration Coefficient Model***

In this study, the filtration function describing the ripening period as proposed by Iwasaki [7] is given as,

$$\lambda(\sigma) = \lambda_0 (1 + \beta \sigma) \quad (6)$$

However, for sake of simplicity it was assumed that the filtration coefficient increased steadily from $\lambda = 0.00$ (cm^{-1}) at t = 0 to a maximum value of $\lambda = 0.02$ (cm^{-1}) at t_{max}.

- ***Porosity reduction model.***

The porosity of a formation increases with increase in the pore pressure according the compressibility model [8]:

$$\phi = \phi_o \left[1 + c_f (p - p_o) \right] \quad (7)$$

- ***Permeability reduction model.***

The permeability of the porous media is calculated from its porosity by using the Kozeny-Carman equation [9], expressed as;

$$k = \frac{\phi^3}{k_z(1-\phi)^2} \tag{8}$$

Where k_z is the kozeny constant given as;

$$k_z = \frac{\phi_i^3}{k_i(1-\phi_i)^2} \tag{9}$$

It is assumed that the nature of the porous media does not change appreciably as a result of particle invasion, so that the kozeny contstant k_z remains unchanged.

- ***Impedance model.***

The impedance model (i.e. inverse of the injectivity decline α) used here was developed in [10] as given below:

$$\frac{1}{\alpha} = \frac{1}{k_D(t)}\left[\frac{\ln\left(\frac{r_f}{r_w}\right)}{\ln\left(\frac{r_e}{r_w}\right)} + \frac{\ln\left(\frac{r_e}{r_f}\right)}{\ln\left(\frac{r_e}{r_w}\right)}\right] \tag{10}$$

$$k_D = \frac{1}{1+\beta c_p(r,t)} \tag{11}$$

$$c_p(r,t) = 0, \ for\ r^2 > {}^{qt}/_{\pi h\phi_m} + r_w^2 \tag{12}$$

$$c_p(r,t) = \lambda c t exp^{[-\lambda\pi(r^2-r_w^2)h\phi_m/q]}, \ for\ r^2 < {}^{qt}/_{\pi h\phi_m} + r_w^2 \tag{13}$$

$$r_f^2 = {}^{qt}/_{\pi h\phi_m} + r_w^2, \ for\ {}^{qt}/_{\pi h\phi_m} < r_e^2 - r_w^2 \tag{14}$$

$$r_f^2 = r_e^2 - r_w^2, \ for\ {}^{qt}/_{\pi h\phi_m} > r_e^2 - r_w^2 \tag{15}$$

- ***Cake thickness equation.***

From the following material balance equation [10],

$$2\pi r_w h e_c(1-\phi_c) = qtC \tag{16}$$

The thickness of the cake matrix fraction Zc can be represented as:

$$Z_c = e_c(1-\phi_c) \tag{17}$$

Hence;

$$Z_c = C\frac{\phi_m r_e}{2r_w}(t_D) \tag{18}$$

Where

$$t_D = \frac{qt}{2\pi r_e^2 h\phi_m} \tag{19}$$

2.0 Numerical Solution

Descritizing equation (1) using the implicit finite difference (FD) scheme, we have:

$$\left[\frac{p_{i+1}^{n+1} - 2p_i^{n+1} + p_{i-1}^{n+1}}{\Delta r^2}\right] + \lambda\left[\frac{p_{i+1}^{n+1} - p_{i-1}^{n+1}}{2\Delta r}\right] = \frac{\phi_m}{D}\left[\frac{p_i^{n+1} - p_i^n}{\Delta t}\right] \tag{20}$$

$$\frac{\Delta t}{\Delta r^2}[p_{i+1}^{n+1} - 2p_i^{n+1} + p_{i-1}^{n+1}] + \frac{\lambda\Delta t}{2\Delta r}[p_{i+1}^{n+1} - p_{i-1}^{n+1}] = \frac{\phi_m}{D}[p_i^{n+1} - p_i^n] \tag{21}$$

$$p_{i-1}^{n+1}\left[\frac{\Delta t}{\Delta r^2} - \frac{\lambda\Delta t}{2\Delta r}\right] - p_i^{n+1}\left[\frac{2\Delta t}{\Delta r^2} + \frac{\phi_m}{D}\right] + p_{i+1}^{n+1}\left[\frac{\Delta t}{\Delta r^2} - \frac{\lambda\Delta t}{2\Delta r}\right] = -\frac{\phi_m}{D}p_i^n \tag{22}$$

Initial conditions:

$p_i^0 = 0$, at time t=0

Boundary conditions:
Dirichlet boundary conditions were assumed i.e.

$p_i^0 = p_{inj}$, i.e constant inlet pressure (injection pressure)

$p_{Nx}^0 = p_0$, constant outlet pressure set as zero

Grid size and time step:
For the range of distance given below,

$0 \leq x \leq 100cm$

The grid size and time step were taken respectively as;

$\Delta r = 10cm.$

$\Delta t = 100days.$

NOTE: it is important to point out that the development of the above model is based on the idea that the filtration coefficient increases steadily during the period of initial filtration, a phenomenon known as filter ripening as noted by **Iwasaki [7].** And as such, it was assumed that the filtration coefficient increased steadily from λ=0.00 (cm^{-1}) at t=0, to a maximum value of λ=0.20 (cm^{-1})at t_{max} in the numerical solution to the model. However, this does not in any way limit the application of the model to any fixed value for λ, as higher values of λ can be accommodated with a marked increase in the model's accuracy by simply reducing the grid size accordingly.

3.0 Formation of Relevant Matrix.

Each of the resulting eleven (11) simultaneous equations below, representing uniform temporal increments in λ by 0.02 (1/cm), where written for the 10 grid blocks to obtain a total of 110 equations that formed eleven (11) ***tridiagonal matrices*** as shown below.

1. $$1.00p_{i-1}^{n+1} - 2.003p_i^{n+1} + 1.00p_{i+1}^{n+1} = -0.003p_i^n \quad (23)$$
2. $$0.90p_{i-1}^{n+1} - 2.003p_i^{n+1} + 1.10p_{i+1}^{n+1} = -0.003p_i^n \quad (24)$$
3. $$0.80p_{i-1}^{n+1} - 2.003p_i^{n+1} + 1.20p_{i+1}^{n+1} = -0.003p_i^n \quad (25)$$
4. $$0.70p_{i-1}^{n+1} - 2.003p_i^{n+1} + 1.30p_{i+1}^{n+1} = -0.003p_i^n \quad (26)$$
5. $$0.60p_{i-1}^{n+1} - 2.003p_i^{n+1} + 1.40p_{i+1}^{n+1} = -0.003p_i^n \quad (27)$$
6. $$0.50p_{i-1}^{n+1} - 2.003p_i^{n+1} + 1.50p_{i+1}^{n+1} = -0.003p_i^n \quad (28)$$
7. $$0.40p_{i-1}^{n+1} - 2.003p_i^{n+1} + 1.60p_{i+1}^{n+1} = -0.003p_i^n \quad (29)$$
8. $$0.30p_{i-1}^{n+1} - 2.003p_i^{n+1} + 1.70p_{i+1}^{n+1} = -0.003p_i^n \quad (30)$$
9. $$0.20p_{i-1}^{n+1} - 2.003p_i^{n+1} + 1.80p_{i+1}^{n+1} = -0.003p_i^n \quad (31)$$
10. $$0.10p_{i-1}^{n+1} - 2.003p_i^{n+1} + 1.90p_{i+1}^{n+1} = -0.003p_i^n \quad (32)$$
11. $$0.00p_{i-1}^{n+1} - 2.003p_i^{n+1} + 2.00p_{i+1}^{n+1} = -0.003p_i^n \quad (33)$$

Writing **Eq. (23)** for example, for each of the ten 10 grid blocks, the resulting matrix would have the form shown below;

$$\begin{pmatrix} a_2 & 1 & 0 & 0 & 0 & 0 & 0 & 0 \\ 1 & a_3 & 1 & 0 & 0 & 0 & 0 & 0 \\ 0 & 1 & a_4 & 1 & 0 & 0 & 0 & 0 \\ 0 & 0 & 1 & a_5 & 1 & 0 & 0 & 0 \\ 0 & 0 & 0 & 1 & a_6 & 1 & 0 & 0 \\ 0 & 0 & 0 & 0 & 1 & a_7 & 1 & 0 \\ 0 & 0 & 0 & 0 & 0 & 1 & a_8 & 1 \\ 0 & 0 & 0 & 0 & 0 & 0 & 1 & a_9 \end{pmatrix} \times \begin{pmatrix} p_2^{n+1} \\ p_3^{n+1} \\ p_4^{n+1} \\ p_5^{n+1} \\ p_6^{n+1} \\ p_7^{n+1} \\ p_8^{n+1} \\ p_9^{n+1} \end{pmatrix} = \begin{pmatrix} -0.003p_2^n - p_1^* \\ -0.003p_3^n \\ -0.003p_4^n \\ -0.003p_5^n \\ -0.003p_6^n \\ -0.003p_7^n \\ -0.003p_8^n \\ -0.003p_9^n - p_{10}^* \end{pmatrix}$$

Where;

$a_i = -2.003$

Therefore, from **Equation (1)** it is clear that the matrix arising from our implicit finite difference method has the following properties:

(i) It is ***tridiagonal*** - that is, it has a maximum of three non-zero elements in any row and these are symmetric around the central diagonal;
(ii) It is very ***sparse*** - that is, most of the elements are zero.
The Thomas Algorithm is a special form of Gaussian elimination that can be used to solve tridiagonal systems of equations.
Hence, for this research, a very simple computational procedure, called the ***Thomas algorithm*** programmed using ***FORTRAN FORCE2.0*** **(See Appendix A)** was used to solve the resulting tridiagonal matrices.

4.0 Results and Discussion.

Using the input parameters **as shown in Table 1** for reservoir/injection well data, the model was run in FORTRAN and the results were generated. **Fig. 1, Fig. 2, Fig. 3, Fig. 4, Fig. 5 and Fig. 6** show the modelled injection pressure decline, formation porosity, permeability, impedance, injectivity decline and cake thickness profiles for the set of parameters including internal and external filtration. Based on the results obtained from the model, the **critical formation porosity Ø*** was obtained as 0.14 at which the filter cake buildup began at a **transition time t_{tr}** of 1000 days.

Table 1: Hypothetical Reservoir/Injection Well Data

K (md)	**40**
C_f (1/pa)	0.000000001
D (cm^2/s)	0.006050
R_e (cm)	200
Porosity	0.2
r_w (cm)	0.02
q (cm^3/day)	1360
C (ppm)	1
Kz	0.00025
λ (1/cm)	0.00-0.2
h, (cm)	30

Table 2: Average Porosity Results

t(d)/r(cm)	ϕ(r=0)	ϕ(r=10)	ϕ(r=20)	ϕ(r=30)	ϕ (r=40)	ϕ(r=50)	ϕ(r=60)	ϕ(r=70)	ϕ(r=80)	ϕ(r=90)	ϕ(r=100)
0	**0.2**	**0.2**	**0.2**	**0.2**	**0.2**	**0.2**	**0.2**	**0.2**	**0.2**	**0.2**	**0.2**
100	**0.2**	**0.1876**	**0.1774**	**0.169**	**0.1621**	**0.1565**	**0.1518**	**0.1479**	**0.1448**	**0.1421**	**0.2**
200	**0.2**	**0.1798**	**0.1663**	**0.1573**	**0.1512**	**0.1472**	**0.1445**	**0.1426**	**0.1414**	**0.1405**	**0.2**
300	**0.2**	**0.1723**	**0.1574**	**0.1494**	**0.145**	**0.1427**	**0.1414**	**0.1407**	**0.1403**	**0.1401**	**0.2**
400	**0.2**	**0.1658**	**0.1511**	**0.1448**	**0.142**	**0.1409**	**0.1404**	**0.1402**	**0.1401**	**0.14**	**0.2**
500	**0.2**	**0.16**	**0.1467**	**0.1422**	**0.1408**	**0.1403**	**0.1401**	**0.14**	**0.14**	**0.14**	**0.2**
600	**0.2**	**0.155**	**0.1438**	**0.1409**	**0.1402**	**0.1401**	**0.14**	**0.14**	**0.14**	**0.14**	**0.2**
700	**0.2**	**0.1506**	**0.1419**	**0.1403**	**0.1401**	**0.14**	**0.14**	**0.14**	**0.14**	**0.14**	**0.2**
800	**0.2**	**0.1467**	**0.1407**	**0.1401**	**0.14**	**0.14**	**0.14**	**0.14**	**0.14**	**0.14**	**0.2**
900	**0.2**	**0.1432**	**0.1402**	**0.14**	**0.14**	**0.14**	**0.14**	**0.14**	**0.14**	**0.14**	**0.2**
T_{tr}=1000	**0.2**	**0.14**	**0.14**	**0.14**	**0.14**	**0.14**	**0.14**	**0.14**	**0.14**	**0.14**	**0.2**
1100	**0.2**	**0.14**	**0.14**	**0.14**	**0.14**	**0.14**	**0.14**	**0.14**	**0.14**	**0.14**	**0.2**

Figure 1 shows the profile of injection pressure variation with time (days), as generated implicitly from the model with a time step Δt of 100days and grid size Δr of 10cm. The plot indicates a gradual decline in injection pressure both radially and temporally as more particles are injected into the porous media.

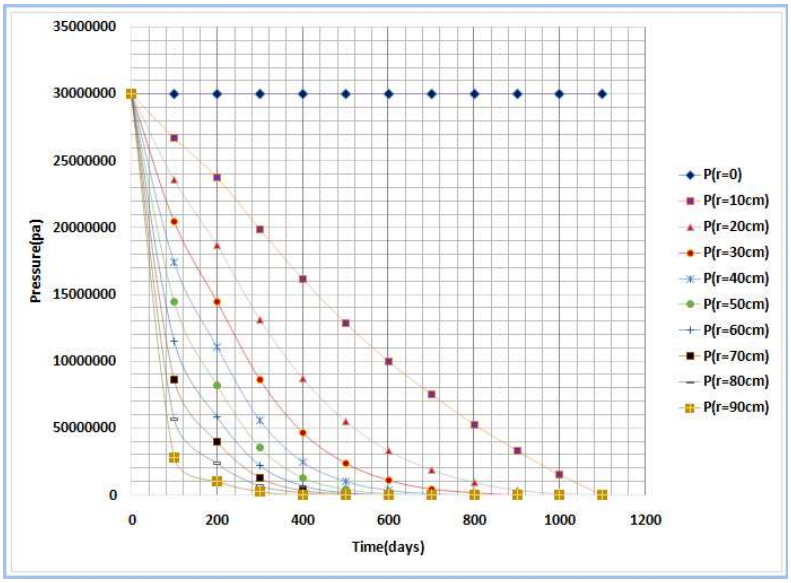

Fig 1: Profile of Injection Pressure as a Function of Time and Radial Distance

Figure 2 shows the variation of average formation porosity with time (days). The plots show a negative slope. This indicates a gradual decline in porosity as more particles are injected into the porous media before and up to the transition time when the filter cake development is initiated resulting in further reduction in permeability and further decline in injectivity.

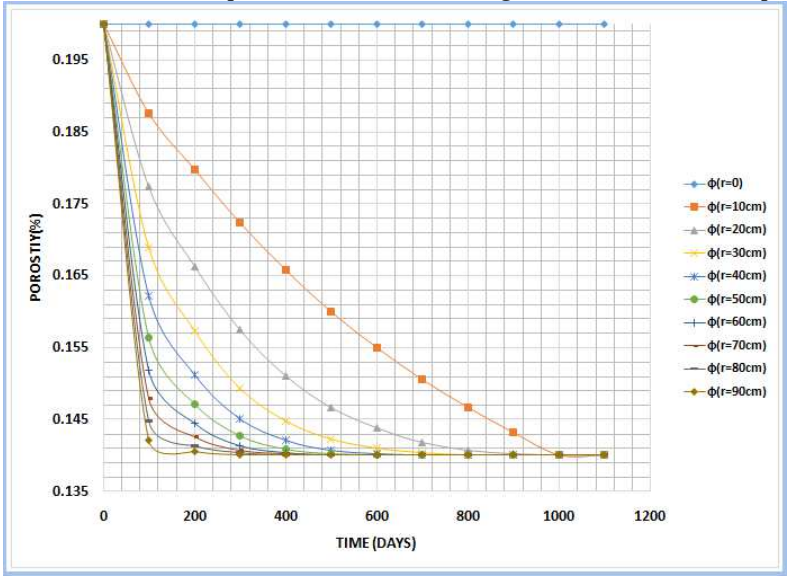

Fig 2: Profile of Average Formation Porosity as a Function of Time and Radius

Figure 3 shows a gradual decline in average formation permeability with time. It is observed that the permeability decreased steadily due to particle invasion around the vicinity of the injection well implying a marked decrease in injectivity due to the reduced porosity and filter cake development both as a function of time and radial distance within the injection interval.

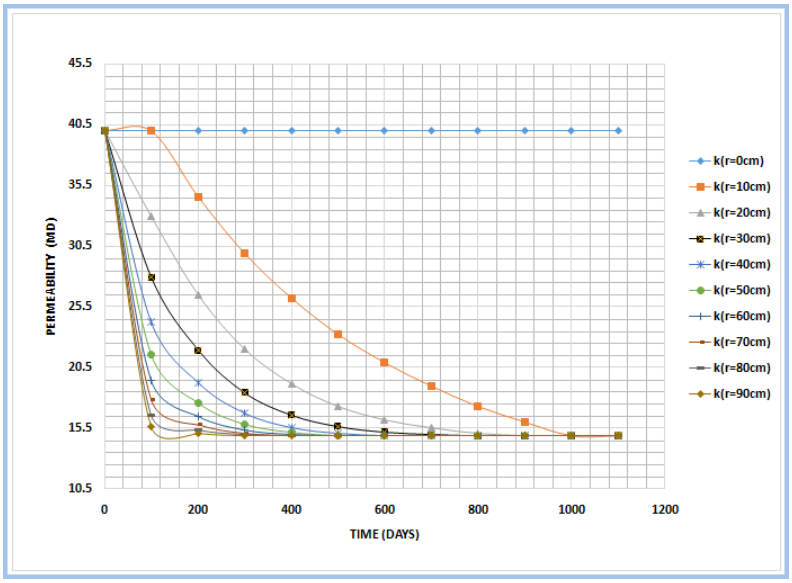

Fig 3: Profile of Average Formation permeability as a Function of Time and Radius

Figure 4 shows the impedance (inverse of injectivity decline α) profile as a function of time, for the water injection program. The steady increase in impedance from 1.0 indicates the effect of particle invasion into the porous media resulting in permeability decreasing steadily around the vicinity of the injection well implying a reduction in injectivity due to the reduced porosity and filter cake development.

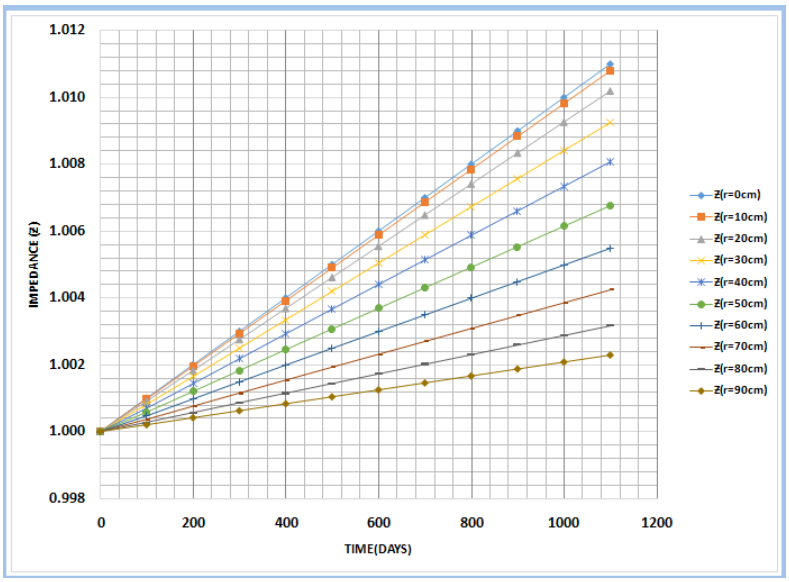

Fig 4: Impedance profile as a Function of Time and Radial distance

Figure 5 shows the injectivity decline (α) profile as a function of time. The steady decrease in injectivity from 1.0 indicates the effect of particle invasion into the porous media resulting in permeability decreasing around the vicinity of the injection well due to the reduced porosity and filter cake development both as a function of time and radial distance.

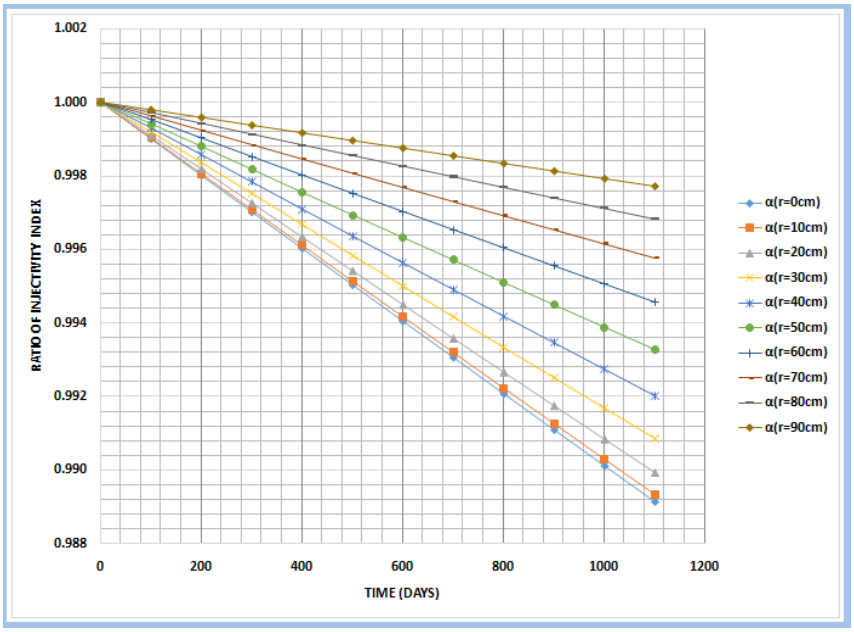

Fig 5: Injectivity Decline Profile as a Function of Time and Radius

Figure 6 is a plot of thickness of the cake matrix fraction Zc (cm) vs time (days), with the positive slope indicating a steady increase in filter cake thickness around the well face leading to more impedance to injectivity and overall injectivity decline.

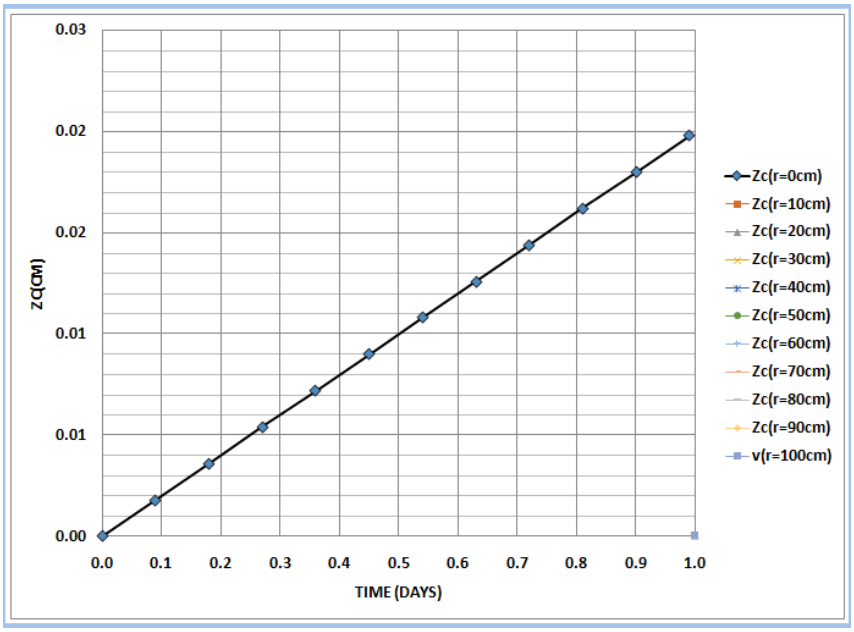

Fig 6: Plot of Thickness of the Cake Matrix fraction Zc vs time

4.0 Conclusion

1. An increase in filter cake thickness and decrease in porosity and permeability was observed with increasing particle invasion from the injected suspension.
2. It has been shown that the model presented [1] is capable of simulating the process of particle invasion in the porous media and the radial model predicted formation damage data agree reasonably well with field observations.
3. The result shows that porosity of the invaded zones reduces with time as against the previous positions by past researchers of an assumed constant porosity [4, 5, 11]
4. The model can be used to improve the accuracy of various existing models in the literature which are based on assumed or constant porosity values.

5.0 Acknowledgment.

The Authors are entirely grateful to the DEPARTMENT OF PETROLEUM ENGINEERING, UNIVERSITY OF BENIN and THE NIGERIAN PETROLEUM DEVELOPMENT COMPANY LTD for being of tremendous support to the successful completion of this work.

6.0 References

[1]. Odeh I.O. and Giegbefumwen P.U.: "A Mathematical Model For The Prediction Of Injectivity Decline," Nigerian Association of Mathematical Physics, Volume 30, May, 2015, pp 413 -420.

[2]. Genuchten, V.M., Wierenga, P.J. 1986." Solute Dispersion Coefficients and Retardation Factors Methods of Soil Analysis, Part-1 "Physical and Mineralogical Methods, 2nd Ed, Agronomy Monograph.9, pp 1025-1054

[3]. Perkins T.K. and Johnston, O.C: " A Review of Diffusion and Dispersion in Porous Media", Society of Petroleum Engineers Journal, SPE 480, pp. 70 - 84

[4]. Rameshchandra Yerramilli.: "Water Injectivity Prediction: Experiments and Modeling," Thesis, Submited To Section of Petroleum Engineering, Dept. of Apllied Earth Sciences, Delft University of Technology, The Netherlands, July 2012.

[5]. Herzig, J.P., Leclerc, D.M. And Goff, P.L.: "Flow of Suspensions through Porous Media-Application to Deep Bed Filtration," Ind. And Eng. Chem. Engrs. Chem., Vol. 62, No. 5, Way 1970, pp 8-34.

[6]. J.E Altoe F. et al.: "Role of Dispersion in Injectivity Impairment: Mathematical and Laboratory Study," SPE 90083 Presented At the Spe Formation Damage Control Symposium Held in Bakersfield, Ca. Sept. 2004.

[7]. Iwasaki, T.: "Some Notes On Sand Filtration," J. Amar. Water Works Asso. Vol. 29, No. 10, 1937, Pp 1591-1602.

[8]. Terek Ahmed: "Reservoir Engineering Hand Book", Third Edition, 2006, pp 254-259.

[9]. Carman, P.C.: "Permeability of Saturated Sands, Soils and Clays," Journal of Agricultural Sciences, Vol. 29, 1939, pp 262-273.

[10]. Shutong Pang and M.M Sharma.: "A Model for Predicting Injectivity Decline in Water Injection Wells," SPE Formation Evaluation Journal, Sept. 1997, pp 194-201

[11]. Bedrikovetsky, P. and Muhammad A.W., Chang G, De Souza A.L.S. and Firtado C.: "Taking Advantage of Of injectivity Decline for sweep Enhancing During waterflood woth Horizontal wells". SPE 122844 ,Presented At the SPE European Formation Damage Conference, Scheveningen, The Netherlands, May 27-29, 2009.

APPENDIX A: FORTRAN PROGRAM FOR THOMAS ALGORITHM

```
C     THOMAS ALGORITHM
C     A MATHEMATICAL MODEL FOR PREDICTING INJECTIVITY DECLINE
DIMENSION      B (25), D (25), A(25), C(25), S(251), P(25), T(25)
       PRINT*, "PUT A VALUE FOR N"
READ (*,*) N
C     FOR INPUT
DO 100 I = 1, N
       PRINT*, "INPUT A VALUE FOR A(I), B(I), C(I), D(I)"
READ (*,*) A(I), B (I), C (I), D(I)
100 CONTINUE
PRINT*,"A(I)          B(I)              C(I)          D(I)"
DO 150 I = 1, N
WRITE (*,*)A(I), B(I), C(I), D(I)
150 CONTINUE
S(1) = D(1)
 T(1) = B(1)
       WRITE (*,*) S(1), T(1)
       DO 200 I = 2,N
       S(I) = D(I) + ((A(I)/T(I-1)) * S(I-1))
  T(I) = B(I) - ((A(I)/T(I-1)) * C(I-1))
       WRITE (*,*) S(I), T(I)
200 CONTINUE
C     ANSWERS
       P(N) = S(N)/T(N)
       WRITE (*,*) P(N)
```

```
J = N
300   J = J - 1
P(J)=   (S(J)/T(J))+ (C(J)/T(J)) * P(J+1)
WRITE (*,*) P(J)
 IF (J.GT.1) GOTO 300
 PAUSE
 STOP
 END.
```